NUMERICAL SIMULATIONS OF INTERACTION OF INVISCID AND VISCOUS INCOMPRESSIBLE FLOW WITH A VIBRATING PROFILE

Radek Honzátko & Jaromír Horáček
Institute of Thermomechanics AS CR, Prague, Czech Republic
Karel Kozel
Dept. of Technical Mathematics, Faculty of Mechanical Engineering, Czech Technical University in Prague, Prague, Czech Republic

ABSTRACT

The work deals with a numerical solution of the interaction of two-dimensional incompressible flows and a freely vibrating profile with large amplitudes. The profile with two degrees of freedom can oscillate around an elastic axis and in the vertical direction. The motion of the profile is described by two nonlinear ordinary differential equations solved numerically using four-order Runge-Kutta method.

The system of incompressible unsteady Euler or Navier-Stokes equations represents the mathematical model of inviscid or viscous flows.

Numerical schemes of the finite volume method are applied on a structured quadrilateral C-mesh. The method of artificial compressibility and a time marching method are used for steady state computations, which precede the unsteady solution. Dual-time stepping method is employed for numerical solution of unsteady simulations.

Deformations of the computational domain due to the profile motion are treated using the Arbitrary Lagrangian-Eulerian method. Numerical scheme used for unsteady flow simulations is implemented in a form satisfying the geometric conservation law.

1. INTRODUCTION

This work is a continuation of previous publications of the authors concerning prescribed oscillations and free vibrations of a profile with one degree of freedom (Honzátko et al., 2006) and two degrees of freedom (Honzátko, 2007) in fluid flow.

Numerical solution of the interaction of incompressible viscous fluid with a vibrating structure with two degrees of freedom based on stabilized finite element method was presented, e.g., in Sváček et al. (2005).

Here, the finite volume method developed for solution of such type of problems is presented.

2. MATHEMATICAL MODEL

The governing equations of viscous flow are two-dimensional incompressible Navier-Stokes equations in dimensionless conservative form (Honzátko, 2007):

$$(\mathbb{D}\mathsf{W})_{\mathsf{t}} + \mathsf{F}^c_{\mathsf{x}} + \mathsf{G}^c_{\mathsf{y}} = \frac{1}{Re}\left(\mathsf{F}^v_{\mathsf{x}} + \mathsf{G}^v_{\mathsf{y}}\right), \qquad (1)$$

where

$$\mathsf{W} = \begin{pmatrix} \mathsf{p} \\ \mathsf{u} \\ \mathsf{v} \end{pmatrix}, \ \mathsf{F}^c = \begin{pmatrix} \mathsf{u} \\ \mathsf{u}^2 + \mathsf{p} \\ \mathsf{uv} \end{pmatrix}, \ \mathsf{G}^c = \begin{pmatrix} \mathsf{v} \\ \mathsf{uv} \\ \mathsf{v}^2 + \mathsf{p} \end{pmatrix}, \qquad (2)$$

$$\mathsf{F}^v = \begin{pmatrix} 0 \\ \mathsf{u}_{\mathsf{x}} \\ \mathsf{v}_{\mathsf{x}} \end{pmatrix}, \ \mathsf{G}^v = \begin{pmatrix} 0 \\ \mathsf{u}_{\mathsf{y}} \\ \mathsf{v}_{\mathsf{y}} \end{pmatrix}, \qquad (3)$$

with diagonal matrix

$$\mathbb{D} = \mathrm{diag}\left(0, 1, 1\right). \qquad (4)$$

Here, W is the vector of conservative variables, F^c, G^c are inviscid physical fluxes and F^v, G^v are viscous physical fluxes. Time is denoted t, space coordinates are represented by x, y and Re is Reynolds number. Symbols $\mathbf{u} = (\mathsf{u}, \mathsf{v})$ and p stand for velocity vector and pressure, respectively.

As far as inviscid flows is concerned, a dimensionless conservative form of incompressible Euler equations can be obtained from equation (1) for $Re \to \infty$:

$$(\mathbb{D}\mathsf{W})_{\mathsf{t}} + \mathsf{F}^c_{\mathsf{x}} + \mathsf{G}^c_{\mathsf{y}} = 0, \qquad (5)$$

where

$$\mathsf{W} = \begin{pmatrix} \mathsf{p} \\ \mathsf{u} \\ \mathsf{v} \end{pmatrix}, \ \mathsf{F}^c = \begin{pmatrix} \mathsf{u} \\ \mathsf{u}^2 + \mathsf{p} \\ \mathsf{uv} \end{pmatrix}, \ \mathsf{G}^c = \begin{pmatrix} \mathsf{v} \\ \mathsf{uv} \\ \mathsf{v}^2 + \mathsf{p} \end{pmatrix}, \qquad (6)$$

with diagonal matrix

$$\mathbb{D} = \mathrm{diag}\left(0, 1, 1\right). \tag{7}$$

The method of artificial compressibility (Chorin, 1967) and a time marching method are used for steady state computations, which precede the unsteady solution. The artificial compressibility method consists in modifying governing equations by adding of the time derivative of pressure to the continuity equation. It is represented by substitution of the matrix $\mathbb{D}$ by the diagonal matrix

$$\mathbb{D}_\beta = \mathrm{diag}\left(\frac{1}{\beta^2}, 1, 1\right). \tag{8}$$

in Eqs. (1) and (5), where $\beta \in \mathbb{R}^+$ is a parameter.

For unsteady flows a dual-time stepping method is applied. The mathematical models are reformulated (Gaitonde, 1998; Arnone et al., 1999, 1993) to be handled by a time-marching steady-state solver. This approach requires the addition of derivatives with respect to a fictious pseudo time τ to each of the three equations (1), resp. (5) to give

$$\mathbb{D}_\beta W_\tau + \mathbb{D} W_{\mathsf{t}} + F^c_{\mathsf{x}} + G^c_{\mathsf{y}} = \frac{1}{Re}\left(\mathsf{F}^v_{\mathsf{x}} + \mathsf{G}^v_{\mathsf{y}}\right), \tag{9}$$

resp.

$$\mathbb{D}_\beta W_\tau + \mathbb{D} W_{\mathsf{t}} + F^c_{\mathsf{x}} + G^c_{\mathsf{y}} = 0. \tag{10}$$

A steady-state solution in pseudo time ($\partial \mathsf{p}/\partial\tau$, $\partial \mathsf{u}/\partial\tau$, $\partial \mathsf{v}/\partial\tau \to 0$) corresponds to an instantaneous unsteady solution in real time t^n, where the superscript n denotes a time level. Hereby, the unsteady flow calculation are transformed into a series of steady-state calculations in pseudo time τ between t^n and t^{n+1}. It provides a possibility to develop a time-accurate time-marching scheme for unsteady incompressible flows.

Upstream condition is represented by prescribed values of the vector $\mathbf{u}$, i. e. $\mathbf{u} = \mathbf{u}_\infty$, pressure is extrapolated from the flow field. The downstream condition is given by a value of p at the outlet boundary, i. e. $\mathsf{p} = \mathsf{p}_{\mathrm{out}}$. The other values of the vector of conservative variables W_{out} at the outlet boundary are extrapolated. Wall conditions are nonpermeability conditions in the case of inviscid flows, i. e. $(\mathsf{u}, \mathsf{v})|^T_{\mathrm{wall}} \cdot \mathbf{n} = (\mathsf{u}_{\mathrm{w}}, \mathsf{v}_{\mathrm{w}})^T \cdot \mathbf{n}$. Here, $(\mathsf{u}_{\mathrm{w}}, \mathsf{v}_{\mathrm{w}})^T$ stands for a velocity vector of the moving boundary and $\mathbf{n}$ designates unit normal vector to the boundary. In the case of viscous flow the non-slip wall boundary condition is used at walls, i. e. $(\mathsf{u}, \mathsf{v})^T|_{\mathrm{wall}} = (\mathsf{u}_{\mathrm{w}}, \mathsf{v}_{\mathrm{w}})^T$.

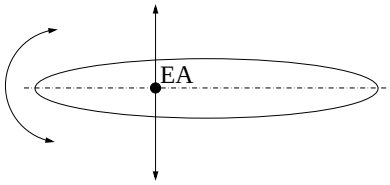

Figure 1: *Schema of the vertical and rotational motion of the profile.*

3. DESCRIPTION OF THE PROFILE MOTION

It is supposed that the vibrating profile has two degrees of freedom. The profile can oscillate in the vertical direction and in the angular direction around a so-called elastic axis EA (see Figure 1). The motion is described by two nonlinear ordinary differential equations:

$$m\ddot{h} + S_\varphi \ddot{\varphi}\cos\varphi - S_\varphi \dot{\varphi}^2 \sin\varphi + \\ + k_{hh} h + d_{hh}\dot{h} = -L(t), \tag{11}$$

$$S_\varphi \ddot{h}\cos\varphi + I_\varphi \ddot{\varphi} + k_{\varphi\varphi}\varphi + d_{\varphi\varphi}\dot{\varphi} = M(t), \tag{12}$$

where, h is vertical displacement of the elastic axis (downwards positive) [m], φ is rotation angle around the elastic axis (clockwise positive) [rad], m is mass of the profile [kg], S_φ is static moment around the elastic axis [kg m], k_{hh} is bending stiffness [N/m], I_φ is inertia moment around the elastic axis [kg m^2] and $k_{\varphi\varphi}$ is torsional stiffness [N m/rad]. The coefficients of the proportional damping are considered in the form $d_{hh} = \varepsilon k_{hh}$ and $d_{\varphi\varphi} = \varepsilon k_{\varphi\varphi}$, where $\varepsilon \in \mathbb{R}$ is a small parameter.

The aerodynamic lift force L [N] acting in the vertical direction (upwards positive) and the torsional moment M [N m] (clockwise positive) in the case of viscous flow are defined as

$$L(t) = -d \oint_{\Gamma_{\mathrm{w}}(t)} \sum_{j=1}^{2} \sigma_{2j} n_j \, dl, \tag{13}$$

$$M(t) = d \oint_{\Gamma_{\mathrm{w}}(t)} \sum_{i,j=1}^{2} \sigma_{ij} n_j r_i^\perp \, dl, \tag{14}$$

where d [m] is the airfoil depth (see Figure 2), $\mathbf{n} = (n_1, n_2)$ is unit inner normal to the profile surface $\Gamma_{\mathrm{w}}(t)$, $\mathbf{r}^\perp = \left(r_1^\perp, r_2^\perp\right) = \left(-\left(y - y^{\mathrm{EA}}\right), x - x^{\mathrm{EA}}\right)$ [m], (x, y) is a point on the profile surface and $\left(x^{\mathrm{EA}}, y^{\mathrm{EA}}\right)$ are coordinates of the elastic axis, and

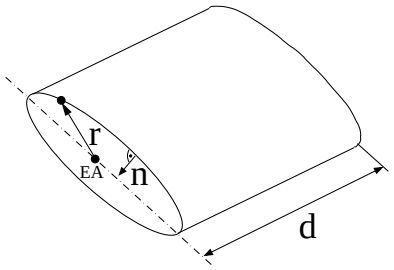

Figure 2: *Schema of the airfoil segment.*

σ_{ij} are components of the stress tensor:

$$\sigma_{11} = -p + 2\rho\nu\frac{\partial u}{\partial x}, \quad \sigma_{22} = -p + 2\rho\nu\frac{\partial v}{\partial y}, \tag{15}$$

$$\sigma_{12} = \sigma_{21} = \rho\nu\left(\frac{\partial u}{\partial y} + \frac{\partial v}{\partial x}\right). \tag{16}$$

Here, ρ [kg m^{-3}] denotes fluid density, p [Pa] is pressure, ν [m^2 s^{-1}] is kinematic viscosity and (u, v) [m s^{-1}] stand for fluid velocity vector components. In the case of inviscid flow, the contribution of viscous forces vanishes and the relations (13) and (14) reduce to

$$L(t) = d\oint_{\Gamma_{\mathrm{w}}(t)} pn_2\,dl, \tag{17}$$

$$M(t) = d\oint_{\Gamma_{\mathrm{w}}(t)} p(-n_2r_1 + n_1r_2)\,dl, \tag{18}$$

where $\mathbf{r} = (r_1, r_2) = (x - x^{\mathrm{EA}}, y - y^{\mathrm{EA}})$ [m].

Eqs. (13), (14) and (17), (18) together with the boundary conditions for velocity on moving boundaries represent the coupling of the fluid with the structure.

The system of Eqs. (11), (12) is completed with the initial conditions prescribing values $h(0)$, $\varphi(0)$, $\dot{h}(0)$, $\dot{\varphi}(0)$. Furthermore, it is transformed to the system of first-order ordinary differential equations and solved numerically by the fourth-order Runge-Kutta method.

4. NUMERICAL SCHEME

Concerning the dual-time stepping method, the derivatives with respect to the real time are discretized using a three-point backward formula, which results in an implicit scheme of second-order of accuracy in time:

$$\begin{aligned}&\mathbb{D}_\beta\left|C_i^{n+1}\right|\frac{\partial \mathsf{W}_i^{n+1}}{\partial\tau} + \\ &+ \mathbb{D}\,\frac{3\left|C_i^{n+1}\right|\mathsf{W}_i^{n+1} - 4\left|C_i^{n}\right|\mathsf{W}_i^{n} + \left|C_i^{n-1}\right|\mathsf{W}_i^{n-1}}{\Delta\mathsf{t}^n} + \\ &+ R_i^c\left(\mathsf{W}^{n+1}\right) - R_i^v\left(\mathsf{W}^{n+1}\right) = 0,\end{aligned} \tag{19}$$

where $R_i^c\left(\mathsf{W}^{n+1}\right)$ and $R_i^v\left(\mathsf{W}^{n+1}\right)$ represent numerical approximations of the relations

$$\frac{1}{\Delta\mathsf{t}^n}\int_{\mathsf{t}^n}^{\mathsf{t}^{n+1}}\left(\oint_{\partial C_i(\mathsf{t})}\left(\mathsf{F}^c d\mathsf{y} - \mathsf{G}^c d\mathsf{x}\right)\right)d\mathsf{t} \tag{20}$$

and

$$\frac{1}{\Delta\mathsf{t}^n}\int_{\mathsf{t}^n}^{\mathsf{t}^{n+1}}\left(\oint_{\partial C_i(\mathsf{t})}\frac{1}{Re}\left(\mathsf{F}^v d\mathsf{y} - \mathsf{G}^v d\mathsf{x}\right)\right)d\mathsf{t}, \tag{21}$$

respectively. Here, C_i^n denotes an i-th finite volume cell $C_i(\mathsf{t})$ at time t^n, $|C_i^n|$ is volume of C_i^n and W_i^n is the approximation of the averaged value of W over C_i^n. The viscous fluxes are neglected for inviscid flow. The convective fluxes are discretized centrally in the finite volume method and an artificial dissipation term is added. The four-stage Runge-Kutta scheme is used for marching in pseudo time τ. The exact numerical discretization and the detailed description of the numerical scheme used is described in Honzátko (2007).

In the ALE formulation the inviscid fluxes are evaluated on the mesh configuration and with grid velocities $\mathbf{w}$ such that a geometric conservation law (LesoinneFarhat, 1996; KoobusFarhat, 1999):

$$|C_i^{n+1}| - |C_i^n| = \int_{\mathsf{t}^n}^{\mathsf{t}^{n+1}}\oint_{\partial C_i(\mathsf{t})}\mathbf{wn}\;d\mathsf{l}\,d\mathsf{t}, \tag{22}$$

is verified. The symbol $\mathbf{n}$ stands for an outer normal vector to the cell boundary.

5. NUMERICAL RESULTS

Numerical results of flow induced vibrations are presented for the profile NACA 0012. A structured quadrilateral C-mesh is used in numerical simulations. The following input quantities were considered (Sváček et al., 2006): $m = 0.086622$ kg, $S_\varphi = -0.000779673$ kg m, $I_\varphi = 0.000487291$ kg m^2, $k_{hh} = 105.109$ N/m, $k_{\varphi\varphi} = 3.695582$ N m/rad, $d = 0.05$ m, $\rho = 1.225$ kg/m^3,

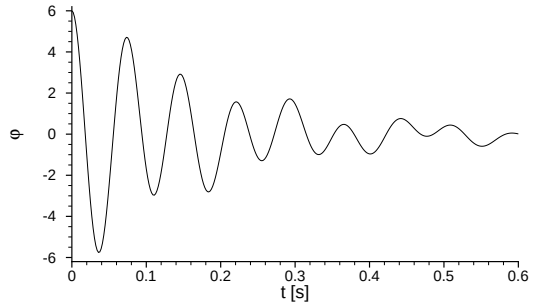

(a) $U_\infty = 5$ m/s

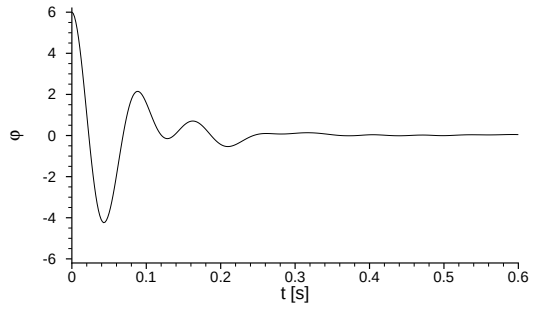

(b) $U_\infty = 25$ m/s

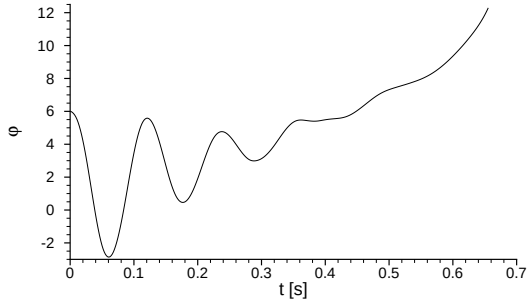

(c) $U_\infty = 41$ m/s

Figure 3: *Angle of profile rotation φ [°] in dependence on time t [s] for upstream flow velocities $U_\infty = 5, 25, 41$ m/s (inviscid flow).*

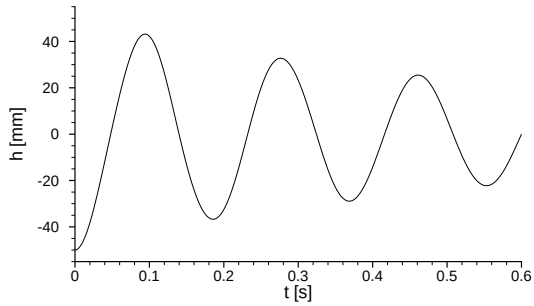

(a) $U_\infty = 5$ m/s

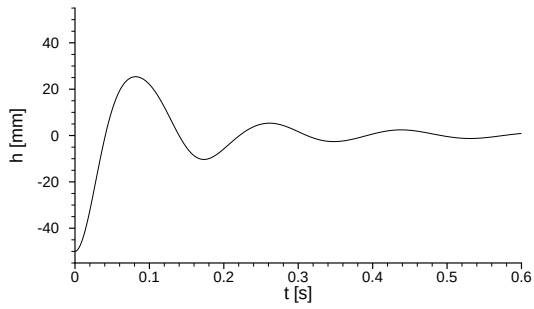

(b) $U_\infty = 25$ m/s

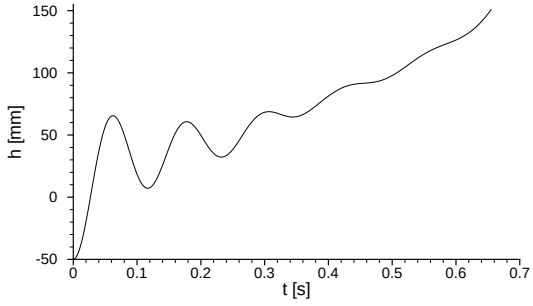

(c) $U_\infty = 41$ m/s

Figure 4: *Vertical profile displacement h [mm] in dependence on time t [s] for upstream flow velocities $U_\infty = 5, 25, 41$ m/s (inviscid flow).*

profile chord $c = 0.3$ m. The position of the elastic axis of the profile measured along the chord from the leading edge is $x_{\mathrm{EA}} = 0.4c = 0.12$ m. The far-field flow velocities $U_\infty = \|\mathbf{u}_\infty\| = 5 - 41$ m/s were considered.

First, the results of numerical simulations of free profile vibrations in inviscid flow are presented. Figures 3 and 4 show the angle of rotation φ [°] and the vertical displacement h [mm] of the profile in dependence on time t [s], respectively. At time $t = 0$, the profile is released with the initial values $h(0) = -0.05$ m, $\dot{h}(0) = 0$, $\varphi(0) = 6°$, $\dot{\varphi}(0) = 0$. The results refer to the upstream flow velocities $U_\infty = 5, 25$ and 41 m/s. For the velocity $U_\infty = 5$ m/s and $U_\infty = 25$ m/s, the system is stable and the free vibrations are damped by aerodynamic forces. For $U_\infty = 41$ m/s an unstable behaviour and a divergence type of instability is observed.

Further, numerical results for inviscid and laminar viscous flows are compared. Figures 5 and 6 show comparison of the angle of rotation φ [°] and vertical displacement h [mm] of the profile in dependence on time t [s] for the upstream flow velocity $U_\infty = 10$ m/s, respectively. Initial conditions are $h(0) = -10$ mm, $\dot{h}(0) = 0$, $\varphi(0) = 3°$, $\dot{\varphi}(0) = 0$.

Isolines of pressure and velocity magnitude around the vibrating profile for laminar viscous flow simulation are shown in Figure 7. The

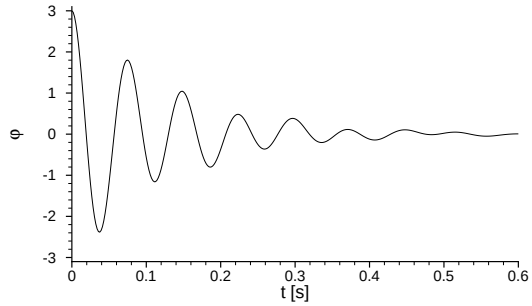

(a) Inviscid flow.

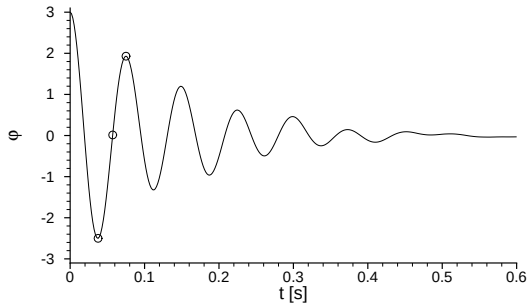

(b) Laminar viscous flow.

Figure 5: *Comparison of inviscid and laminar viscous flow results for angle of rotation φ [°] in dependence on time t [s] ($U_\infty = 10$ m/s).*

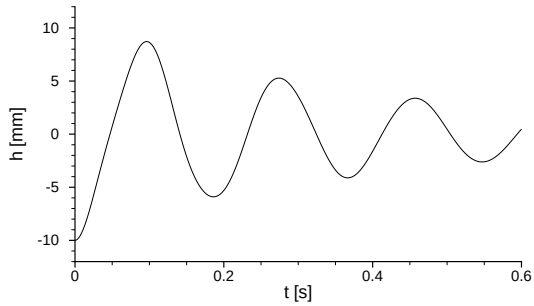

(a) Inviscid flow.

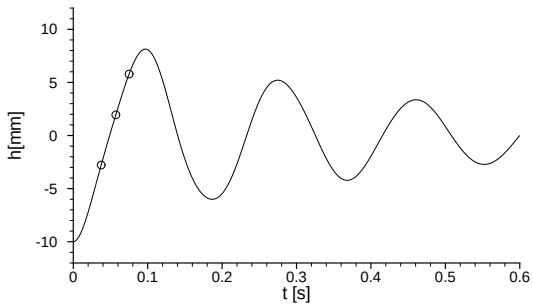

(b) Laminar viscous flow.

Figure 6: *Comparison of inviscid and laminar viscous flow results for vertical displacement h [mm] in dependence on time t [s] ($U_\infty = 10$ m/s).*

fluid flow patterns correspond to time instants $t = 0.04$, 0.06 and 0.08 s, for which the angles of rotation φ and vertical displacements h are marked by circle symbols in Figures 5(b) and 6(b).

6. CONCLUSION

The numerical solver using finite volume method for simulations of interaction of inviscid and laminar viscous incompressible flows and a freely vibrating profile with two degrees of freedom was developed. The numerical calculations for inviscid flow performed with the smaller far-field velocities give expected results for angle and vertical displacements of the profile in time domain, i.e., the damping increases with increasing the upstream flow velocity. The instability of the system was observed for the far-field velocities above the critical one (here represented by $U_\infty = 41$ m/s). The solution is in agreement with the numerical results presented in Sváček et al. (2006), where for the divergence instability is given $U_\infty = 37.7$ m/s and for flutter $U_\infty = 42.4$ m/s computed by NASTRAN code (ČečrdleMaleček, 2002) for linear approximation.

Also first results for laminar viscous flows show expected angle and vertical displacements of the profile in time domain, comparable to the inviscid solution because of small effects of viscous forces for small upstream flow velocities.

6.1. Acknowledgement

This work has partly been supported by the Research Plan of the Ministry of Education of the Czech Republic No 6840770010 and project of the Grant Agency of the Academy of Science of the Czech Republic No IAA200760613 “Computer modelling of aeroelastic phenomena for real fluid flowing past vibrating airfoils particularly after the loss of system stability”.

7. REFERENCES

Arnone, A., Liou, M. S., Povinelli, A. L. (1993). Multigrid time-accurate integration of Navier-Stokes equations. In *AIAA Paper 93-3361.*

Arnone, A., Marconcini, M., Pacciani, R. (1999). On the use of dual time stepping in unsteady tur-

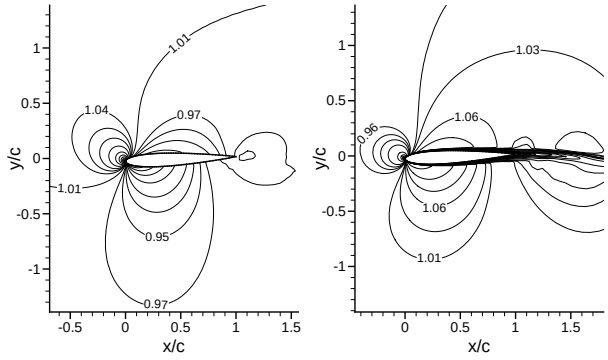

(a) $\varphi = -2.50°$, $h = -2.78$ mm

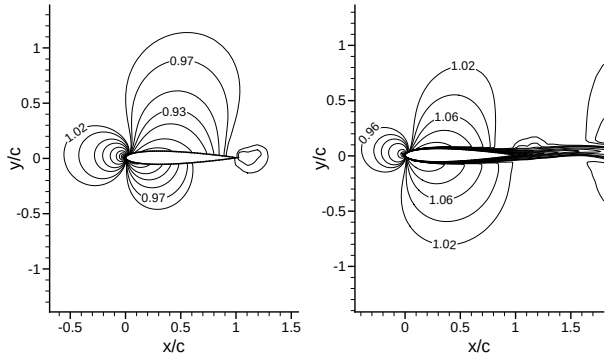

(b) $\varphi = 0.01°$, $h = 1.95$ mm

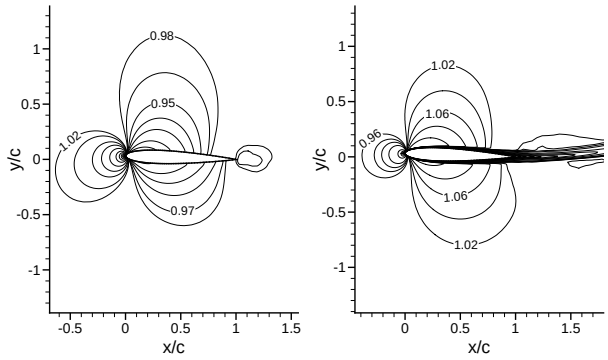

(c) $\varphi = 1.93°$, $h = 5.79$ mm

Figure 7: *Laminar viscous flow simulations, isolines of pressure (left panel) and velocity (right panel) field around the vibrating profile NACA 0012,* $(u_\infty, v_\infty) = (10, 0)$ *m/s.*

bomachinery flow calculations. In *ERCOFTAC Bulletin*, number 42, pages 37–42.

Chorin, A. J. (1967). A numerical method for solving incompressible viscous flow problems. *Journal of Computational Physics*, **2**(1), 12–26.

Gaitonde, A. L. (1998). A dual-time method for two-dimensional unsteady incompreessible flow calculations. *International journal for numerical methods in engineering*, **41**, 1153–1166.

Honzátko, R. (2007). *Numerical Simulations of Incompressible Flows with Dynamical and Aeroelastic Effects.* PhD dissertation, Czech Technical University in Prague, Faculty of Nuclear Sciences and Physical Engineering, Department Mathematics.

Honzátko, R., Kozel, K., Horáček, J. (2006). Numerical solution of 2D incompressible flow over a vibrating airfoil. In *CMFF'06 Conference Proceedings*, pages 233–240, Budapest. Budapest University of Technology and Economics, Department of Fluid Mechanics.

Koobus, B., Farhat, C. (1999). Second-order time-accurate and geometrically conservative implicit schemes for flow computations on unstructured dynamic meshes. *Computer methods in applied mechanics and engineering*, **170**, 103–129.

Lesoinne, M., Farhat, C. (1996). Geometric conservation laws for flow problems with moving boundaries and deformable meshes, and their impact on aeroelastic computations. *Computer methods in applied mechanics and engineering*, **134**, 71–90.

Sváček, P., Feistauer, M., Horáček, J. (2005). Numerical modelling of flow induced airfoil vibrations problem. In *International Conference on Innovation and Integration in Aerospace Sciences [CD - ROM]*, page 10, Belfast. CEIAT, Queen's University Belfast.

Sváček, P., Feistauer, M., Horáček, J. (2006). Numerical simulation of flow induced airfoil vibrations with large amplitudes. *Journal of Fluids and Structures.* DOI 10.1016/j.jfluidstructs.2006.10.005.

Čečrdle, J., Maleček, J. (2002). Verification FEM model of an aircraft construction with two and three degrees of freedom. Technical report R-3418/02, Aeronautical Research and Test Institute, Prague, Letňany. (in Czech).